Optical Society of America. Evan Lally, Jianmin Gong, and Anbo Wang, "Method of multiple references for 3D imaging with Fourier transform interferometry," Opt. Express 18, 17591-17596 (2010). doi: 10.1364/OE.18.017591

Method of multiple references for 3D imaging with Fourier transform interferometry

Evan Lally,* Jianmin Gong, and Anbo Wang

Center for Photonics Technology, Bradley Department of Electrical and Computer Engineering, Virginia Polytechnic Institute and State University, Blacksburg, VA 24061-0111, USA

**evlally@vt.edu*

Abstract: This letter presents an improved phase referencing technique, called Method of Multiple References, for optical profilometry. Based on a lookup table, the method eliminates several major drawbacks of single-reference Fourier Transform Interferometry by enabling surface error correction for steep slopes and step discontinuities, and by allowing mapping of multiple discrete objects using a single image set. The algorithm is tested using a fiber optic coupler-based FTI system and shown to have RMS surface error less than 0.03mm.

OCIS codes: (110.2350) Fiber optics imaging, (110.2650) Fringe analysis, (110.3175) Interferometric imaging, (110.6880) Three-dimensional image acquisition.

References and links

1. F. Chen, G. Brown, and M. M. Song, "Overview of three-dimensional shape measurement using optical methods," Opt. Eng. **39**(1), 10–22 (2000).
2. T. L. Pennington, H. Xiao, R. May, and A. Wang, "Miniaturized 3-D surface profilometer using a fiber optic coupler," Opt. Laser Technol. **33**(5), 313–320 (2001).
3. M. Takeda, and K. Mutoh, "Fourier transform profilometry for the automatic measurement of 3-D object shapes," Appl. Opt. **22**(24), 3977–3982 (1983).
4. T. Judge, "A review of phase unwrapping techniques in fringe analysis," Opt. Lasers Eng. **21**(4), 199–239 (1994).
5. T. L. Pennington, "Miniaturized 3-D Mapping System Using a Fiber Optic Coupler as a Young's Double Pinhole Interferometer," PhD, Electrical Engineering, Virginia Tech, Blacksburg (2000).
6. D. C. Ghiglia, G. A. Mastin, and L. A. Romero, "Cellular-automata method for phase unwrapping," J. Opt. Soc. Am. A **4**(1), 267–280 (1987).
7. J. M. Huntley, "Noise-immune phase unwrapping algorithm," Appl. Opt. **28**(16), 3268–3270 (1989).
8. H. E. Cline, W. E. Lorensen, and A. S. Holik, "Automatic moire contouring," Appl. Opt. **23**(10), 1454–1459 (1984).
9. H. O. Saldner, and J. M. Huntley, "Profilometry using temporal phase unwrapping and a spatial light modulator-based fringe projector," Opt. Eng. **36**(2), 610–615 (1997).
10. K. Itoh, "Analysis of the phase unwrapping algorithm," Appl. Opt. **21**(14), 2470 (1982).
11. W. W. Macy, Jr., "Two-dimensional fringe-pattern analysis," Appl. Opt. **22**(23), 3898–3901 (1983).

1. Introduction

Fourier Transform Interferometry (FTI) is a powerful technique for non-contact surface profilometry that offers high resolution using only one or two images [1]. An interference fringe pattern, often generated with a fiber optic coupler [2], is projected onto an object, and the FTI algorithm converts the spatially-varying phase of the projected interferogram into a continuous 3D surface map [3].

Phase unwrapping plays a critical role in the surface reconstruction process and has therefore attracted a great deal of attention [4]. In past work, a single reference fringe was used to measure absolute interferogram phase [3,5]. Others have acknowledged the problem of error propagation and have developed a variety of solutions to handle point errors when unwrapping from a single reference [6,7]. Unfortunately, these techniques are unable to handle discontinuities that extend the entire length of the surface.

In this letter, a new technique is proposed that allows the specification of an arbitrary reference fringe. This Method of Multiple References (MoMR) removes the limitations associated with fixed-fringe referencing, enabling imaging of multiple discrete surfaces,

#126043 - $15.00 USD Received 25 Mar 2010; revised 3 Jun 2010; accepted 28 Jun 2010; published 2 Aug 2010

eliminating limitations on object placement, and providing a means for surface error correction. Unlike temporal or phase shifting techniques [8,9], MoMR realizes these improvements using the simplified fiber coupler-based system geometry shown in Fig. 1.

2. Motivation: FTI referencing and limitations

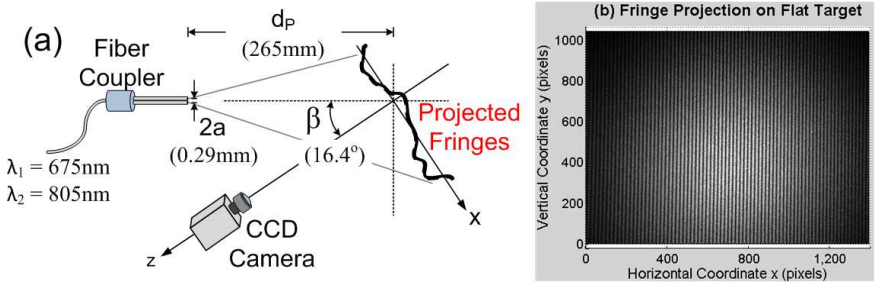

Fig. 1. (a) Schematic of fiber the coupler-based Fourier Transform Interferometry setup used in this demonstration. (b) Image of fringes projected onto a flat calibration target.

FTI begins with the projection of interference fringes on an unknown surface (Fig. 1). The intensity of each interferogram row is a sinusoid with spatially varying phase $\varphi(x,z)$. This phase is governed by the geometry of the system, including the illumination wavelength λ, pinhole spacing $2a$, projection angle β, and the pinhole-to-surface distance d_P [2].

$$\varphi(x,z) = \frac{4\pi a}{\lambda} \times \frac{z(x)\sin\beta + x\cos\beta}{d_P + x\sin\beta - z(x)\cos\beta} \tag{1}$$

The phase is extracted from a 2D image by taking the row-by-row fast Fourier transform (FFT), using a single-sideband filter and inverse FFT to extract the complex envelope $c(x)$ [3]. From Eq. (2), it is clear that the extracted phase is bounded by +/–π, requiring an unwrapping step to convert it to a continuously increasing function. There exists a variety of well-proven phase unwrapping techniques [10,11], but in practice, the result is un-referenced. There is no inherent indication of the location of the $\varphi = N\cdot 2\pi$ point corresponding to the N^{th} order fringe.

$$\varphi(x) = \tan^{-1}\left[\mathrm{Im}\{c(x)\}/\mathrm{Re}\{c(x)\}\right] \tag{2}$$

The nonlinear dependence of $\varphi(x,z)$ requires knowledge of the absolute phase to reconstruct a surface map $z(x)$ [3,9]. Traditionally, the zero-order fringe ($\varphi = 0$) is used as a reference for the final surface reconstruction step [3]. This fringe represents the set of points that are equidistant from the dual-pinhole source. It is easy to find using a second reference image, containing fringes produced at a different wavelength [5]. Such use of a single, fixed reference fringe carries two major limitations: (a) inability to map multiple discontinuous surfaces, and (b) error propagation. Both problems are solved through the use of MoMR.

3. Method of multiple references (MoMR)

MoMR is a simple technique that remedies both of the major fixed-reference FTI limitations. As in zero-order referencing, two images are collected at different illumination wavelengths, λ_1 and λ_2 [5]. MoMR, however, does not focus on a single fringe. Instead, it provides a means to uniquely identify the order of any fringe, projected on an unknown surface, so it may be used as a reference. In this way, the fringe pattern contains multiple references: any fringe peak could be used to determine absolute phase from the unwrapped phase map.

3.1 Initial Calibration

FTI calibration involves imaging sets of fringes projected onto an optically flat target. During system calibration, the exact horizontal pixel location of every fringe peak in the image is determined for each row using a localized curve fitting technique. These row-by-row peak

#126043 - $15.00 USD Received 25 Mar 2010; revised 3 Jun 2010; accepted 28 Jun 2010; published 2 Aug 2010

positions are then averaged to compute a single horizontal peak location x_0 for each vertical fringe. The entire calibration process is repeated at 19 different target heights over the range of Δz = 25mm. From this one-time calibration, a lookup table (illustrated in Fig. 2) is created that enables identification of any fringe in subsequent unknown surface images.

Fringe order is uniquely determined by two key parameters measured during calibration: (a) the position of the peak in the main image $x_0(\lambda_1)$, and (b) the difference between its locations at the two projection wavelengths $\Delta x_0 = x_0(\lambda_1) - x_0(\lambda_2)$. Each fringe has a unique combination of $x_0(\lambda_1)$ and Δx_0 that differentiates it from the other fringes.

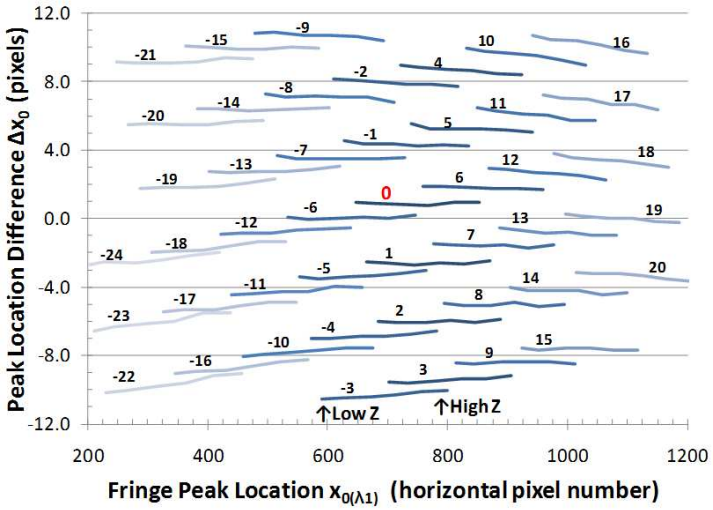

Fig. 2. Graphical representation of lookup table for MoMR, based on data taken from calibration of the fiber optic coupler-based FTI system in Fig. 1. The value of $x_0(\lambda_1)$ varies as the surface height is changed, but the peak difference Δx_0 remains relatively constant. Nominal fringe orders, assigned during calibration, are listed above each data line.

3.2 Application during Imaging

The determination of fringe order, which is performed automatically using the MoMR lookup table, allows any fringe to be used as the reference. Images of fringes projected on an unknown surface are collected, and an arbitrary N^{th} fringe is selected as the reference. The MoMR algorithm computes $x_0(\lambda_1)$ and Δx_0 for the selected fringe and compares their values to the lookup table in Fig. 2 to determine the fringe order N. Next, the algorithm shifts the unwrapped phase $\varphi_U(x,y)$ to equal $N \cdot 2\pi$ at pixel x_0 by applying a phase shift $\varphi_S(y)$ to each row.

$$\begin{aligned} \varphi_S^{(N)}(y) &= \varphi_U\left(x_0(y), y\right) - N \cdot 2\pi \\ \varphi_{ref:N}(x, y) &= \varphi_U\left(x, y\right) - \varphi_S^{(N)}(y) \end{aligned} \tag{3}$$

4. MoMR usage and results

4.1 Multi-surface imaging

Every image row to be processed must contain a reference point. Using traditional fixed-fringe referencing, this necessitates placement of the object directly under a pre-determined location. Irregularly shaped surfaces must be carefully oriented so that information is not lost at the upper and lower boundaries of the object. Multiple objects are impossible to image with a fixed reference because at most, the reference fringe is projected on only one surface (Fig. 3a). Use of MoMR, eliminates these problems by allowing selection of multiple reference fringes based on surface geometry and placement.

#126043 - $15.00 USD Received 25 Mar 2010; revised 3 Jun 2010; accepted 28 Jun 2010; published 2 Aug 2010

The multi-surface capability of MoMR is demonstrated by imaging three small limestone particles, roughly 1-2cm in size (Fig. 3b), placed on a black matte background for contrast-based windowing. Had they been placed on a reflective background, the edges of each particle would present un-recoverable features for fixed-reference FTI (in prior work, the target was embedded in the mat itself [3]). Three reference fringes are used in the processing, one for each of the discrete surfaces. A boundary definition step is used to remove steep slope errors at the edges of the particles, leaving the majority of their surfaces well-mapped.

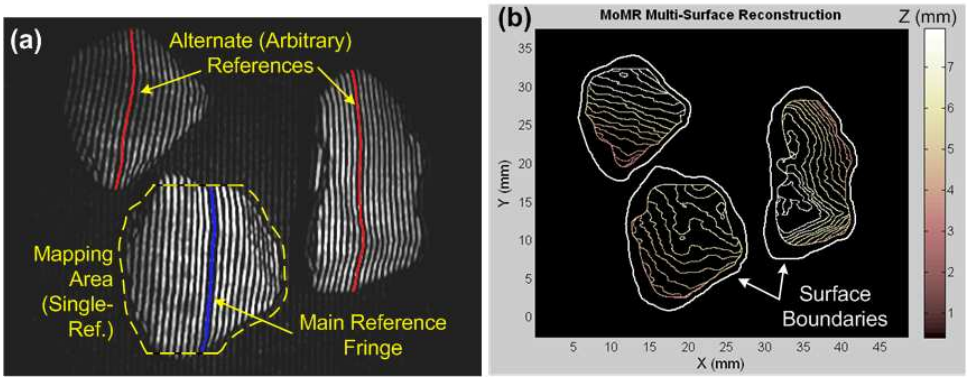

Fig. 3. (a) Interferogram projection on a multi-surface image. A single fixed reference fringe and its resulting limited mapping area are shown, as are the multiple alternate references allowed by MoMR. (b) Contour map demonstrating multi-surface reconstruction. Limestone particles (same as (a)) are bounded and profiled using 3 reference fringes.

4.2 Surface error correction

Applying a reference fringe is akin to unwrapping outward from the reference point in both directions. During phase unwrapping, errors that occur in the surface reconstruction tend to propagate away from the reference point along the rows in which they occur. In this way, single point errors in the phase map can ruin large areas of otherwise good data (this effect is evident in Fig. 6).

The majority of surface errors are caused by two specific conditions, both related to the FTI filtering step: steep slopes and step discontinuities. Steep slope errors can be understood by considering the instantaneous spatial frequency of a single interferogram row $f(x)$, which is derived from Eq. (1) under the assumption that $d_P >> x, z$. From Eq. (4), it is clear the fringe frequency at each point along a data row is modulated by the surface slope at that point, dz/dx. Steep slopes generate a wider bandwidth signal, which is attenuated by the FTI filter and therefore has reduced SNR (Fig. 4), contributing to noise-induced errors in the surface map.

$$f(x) = \frac{1}{2\pi}\frac{d\varphi}{dx} \approx \frac{2a}{\lambda d_P}\left[\cos\beta + \frac{dz}{dx}\sin\beta\right] \tag{4}$$

A step discontinuity is a special case in which dz/dx is nearly infinite. The maximum discontinuity Δz_{max} occurs at a phase jump of $\Delta\varphi/\Delta x > 2\pi$ over $\Delta x = 1$ pixel. This is shown in Eq. (5), where $S_{mm} = 28.2$ pixels/mm is the horizontal scale of the system. This type of error is not noise-induced. Instead, large step discontinuities simply cause the FTI algorithm to lose track of the correct phase, assigning an incorrect fringe order after the discontinuity.

$$\Delta z_{\max} = \frac{\lambda d_P}{2a\sin\beta} - \frac{1}{S_{mm}}\cot\beta \quad = \quad 2.1mm \tag{5}$$

#126043 - $15.00 USD Received 25 Mar 2010; revised 3 Jun 2010; accepted 28 Jun 2010; published 2 Aug 2010

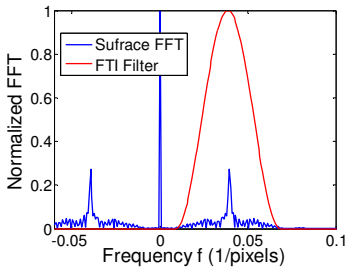

Fig. 4. Simulated two-sided FFT of a single data row containing a localized 2:1 slope. A Hann window, symmetric about the center frequency of the fringe pattern, is used as the FTI filter. The presence of the steep slope adds wide sidebands to the center carrier, and portions of the signal are attenuated by the edges of the filter.

MoMR allows the same image to be processed multiple times using different reference fringes, providing a means of eliminating error propagation through detection and correction of bad data regions. If two reference fringes, M^{th} and N^{th} order, are selected, their phase shift vectors $\varphi_S^{(N)}(y)$ and $\varphi_S^{(M)}(y)$, defined in Eq. (3), can be compared to identify rows that contain erroneous data. Because MoMR simply uses different reference fringes to generate the same master-referenced phase map, $\varphi_S(y)$ should be the same regardless of the reference chosen, and nonzero values of φ_{err} in Eq. (6) can be used to locate errors on unknown surfaces.

$$\varphi_{err}(y) = \varphi_S^{(N)}(y) - \varphi_S^{(M)}(y) \tag{6}$$

Once erroneous rows have been identified, the horizontal propagation of errors can be eliminated by selective replacement of the unwrapped phase. For each row in which $\varphi_{err} > 0$, the algorithm must determine the horizontal ranges over which to adopt the phase data referenced to the N^{th} and M^{th} fringes. On irregular surfaces, this is done by comparing the phase map of the bad row with the phase in an adjacent error-free row (Fig. 5a). On the highly regular test surface shown in Fig. 6, all rows contain propagating errors, and the boundaries of each region of data are located based on the slope of the reconstructed surface profile $z(x)$ for each reference (Fig. 5b). In either case, the error-inducing surface feature is isolated through the use of different reference fringes located on either side. In this way, MoMR eliminates the propagation of errors caused by phase unwrapping.

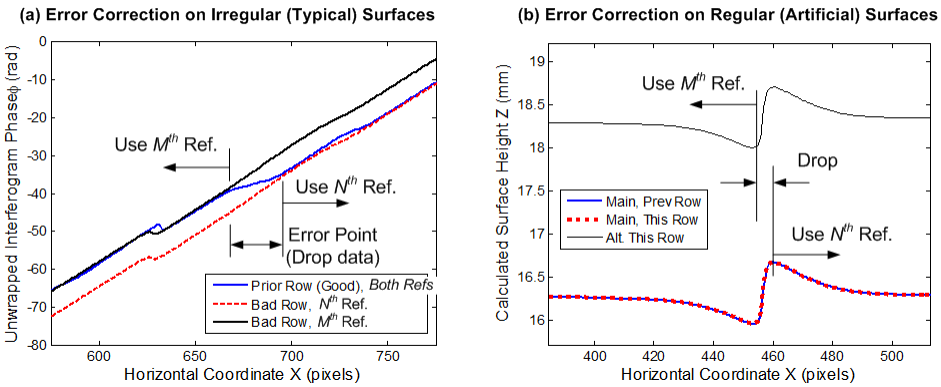

Fig. 5. Determination of data ranges for MoMR surface error correction. Each reference fringe is attributed to a region of data on one side of an error feature, eliminating the propagation of errors. Reference regions are determined by (a) comparison with an adjacent error-free row, or (b) identification of discontinuities from the slope of the reconstructed surface map. The majority of real surfaces fall into case (a), but (b) applies to the test surface in Fig. 6.

To demonstrate MoMR for surface error correction, a test target with a 2mm/60° slope and step discontinuity of −6mm is machined and painted. Images of the fringe patterns projected

#126043 - $15.00 USD Received 25 Mar 2010; revised 3 Jun 2010; accepted 28 Jun 2010; published 2 Aug 2010

on the target are collected, and processed using the $N_0 = -5$ fringe in the center of the target as the primary reference.

Results from this first processing step illustrate the limitations of fixed-fringe referencing (Fig. 6a). The region in the neighborhood of the reference fringe is reconstructed properly, but the steep slope and step discontinuity cause errors that propagate to the left and right sides of the image. The row-to-row variations on the left side are typical of noise-limited steep slope errors in which dz/dx is near the edge of the filter passband. The $\Delta z = -6$mm step on the right side of the image is not recognized because it exceeds $\Delta z_{max} = 2.1$mm [Eq. (5)].

Error correction is performed by re-processing the same data set using two additional reference fringes, $N_1 = -23$ and $N_2 = 19$, located in the left (upper) and right (lower) regions, respectively. The resulting corrected surface map (Fig. 6b) shows that, although the FTI system cannot reconstruct steep slopes or step discontinuities, the MoMR correction technique can prevent these features from obscuring otherwise accurate surface data in other regions. To confirm the accuracy of the technique, measurements of the target are taken using a micrometer with 10μm resolution and compared to the surface map in each region (Table 1).

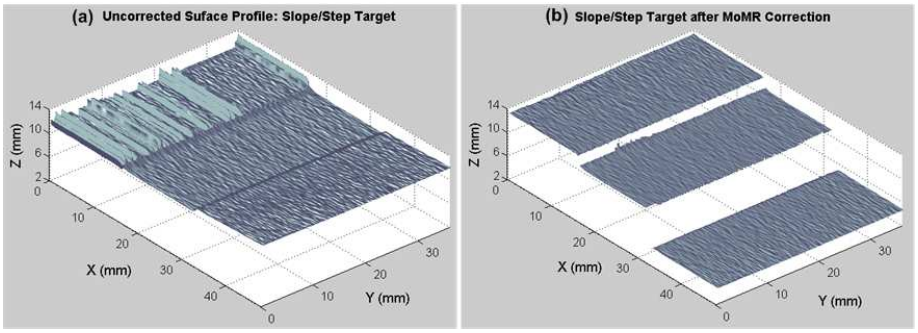

Fig. 6. (a) Uncorrected surface profile after initial processing with reference fringe located in center region (equivalent to fixed fringe referencing). (b) Surface profile after MoMR correction. The areas to the left of the steep slope (upper) and right of the step discontinuity (lower) are now correctly represented.

Table 1. Comparison to physical measurement: MoMR-FTI accuracy and resolution

all units in mm	Upper (L)	Center	Lower (R)
Mean Z (Physical)	13.17	11.11	4.93
Mean Z (FTI-MoMR)	13.19	11.12	4.91
2σ Resolution (FTI-MoMR)	0.022	0.018	0.025
RMS Error (FTI-MoMR)	0.024	0.016	0.030

5. Conclusion

The Method of Multiple References is a novel technique for processing of optical surface profilometry data designed to augment a well-established technology: Fourier Transform Interferometry. It represents an improvement over conventional fringe referencing techniques and a significant departure from prior strategies for error mitigation through phase unwrapping. MoMR is compatible with any FTI system geometry, allowing the system to be scaled for potential applications including inspection of particles, MEMS devices, turbine components, microelectronic circuit boards, and many others.

Acknowledgements

The authors would like to thank Matthias Hofmann and Jihaeng Yi of the Bradley Department of Electrical and Computer Engineering, Virginia Tech, for their help in manufacturing the fiber coupler fringe source. They also thank Dr. Linbing Wang of the Via Department of Civil and Environmental Engineering, Virginia Tech, for his support and advice. This work was supported by the National Cooperative Highway Research Program under Project 04-34.

#126043 - $15.00 USD Received 25 Mar 2010; revised 3 Jun 2010; accepted 28 Jun 2010; published 2 Aug 2010